European Conerence on Severe Storms 2015,
14–18 September 2015, Wiener Neustadt, Austria, ECSS2015-67-2

An Extended Perspective for DMC Initiation in the Alpine Region?

Thomas Krennert[1], Astrid Kainz[1,2], Stefano Serafin[2]
(1) ZAMG, Central Institute of Meteorology and Geodynamics, Hohe Warte 39, A – 1190 Vienna, t.krennert@zamg.ac.at
(2) Department of Meteorology and Geophysics, University of Vienna, Althanstraße 14, A – 1090 Vienna , Austria

Introduction

Predicting the exact initiation, intensity and propagation of thunderstorms and convective complexes remains a challenge to operational forecasters, in particular in the presence of orography, in the absence of fronts and when a forecast lead time of more than three hours is desired. Single-cell or pulse convection, developing without fronts, represents about 30% of the summertime convection in the Eastern Alpine region (Krennert et al., 2003).
In a simulation with the WRF model for the case of 7 July 2014, the evolution of Deep Moist Convection (DMC) occurs in conjunction with a significant increase in the vertical wind shear and in the horizontal and vertical gradients of Equivalent Potential Temperature Θ_e in the vicinity of an Upper Tropospheric Moisture Gradient (UTMG). Hence, the coexistence of moist gravitational and moist symmetric instabilities along the UTMG seems plausible.

A hypothesis linking UTMG with probable additional lift for DMC initiation

Studies of satellite imagery of cases with similar synoptic conditions showed that UTMG are often favourable locations for the initial evolution from shallow to deep moist convection (Krennert, et al. 2003; see e.g. Fig.1, a-c).

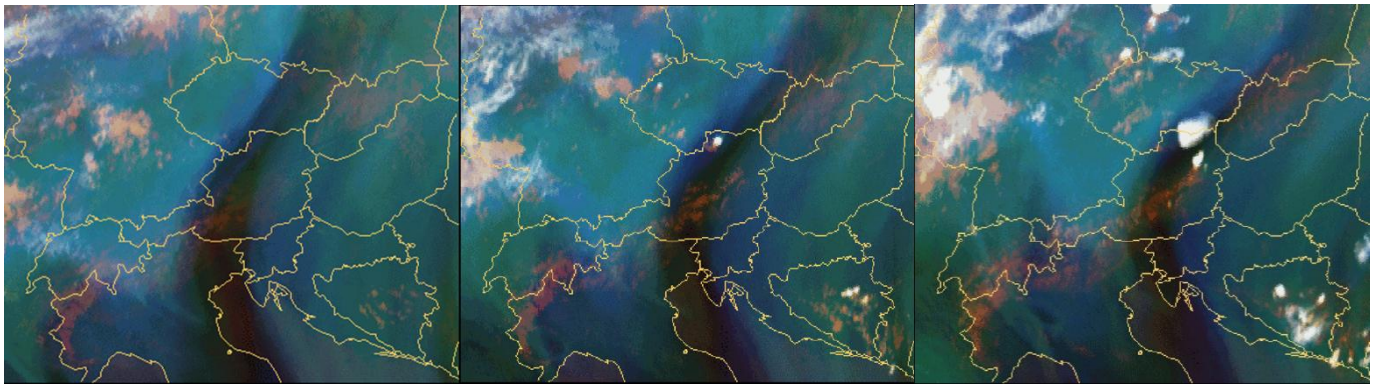

Fig. 1, a-c: Convective initiation along an UTMG over north eastern Austria, 28 July 2005, 1100, 1200 and 1300 UTC, MSG RGB Image composite: Low Clouds: IR 8.7µm (red); Mid Level Moisture: WV 7.3µm (green); High level Moisture: WV 6.2µm (blue)

According to Markowski et al., 2010, DMC is initiated when a rising (and saturated) air parcel reaches its Level of Free Convection (LFC). Given sufficient moisture supply to resist cloud detrainment, mostly from lower atmospheric levels, the air parcel will then rise until its buoyancy is consumed and its properties are again the same as the surrounding air (e.g. at the Equilibrium Level, EL).
Except in the case of the so-called elevated convection, DMC is usually surface-based: buoyant plumes rise from within the boundary layer due to well-known mechanisms, e.g. convergence or buoyant updrafts from overheated areas or mountain slopes. If these air parcels reach their Lifting Condensation Level (LCL), a widespread formation of shallow convective clouds (rising up to 850 or 700 hPa) takes place, for instance above mountainous areas of the Alps and the surrounding pre–alpine regions. This is a common occurrence within synoptic settings with low horizontal pressure gradients and the absence of fronts (Krennert et al., 2003). Often, air parcels are prevented from reaching

their LFC by capping inversions (Convective Inhibition, CIN), the lack or weakening of the necessary ingredients, as well as cloud detrainment in a dry mid-level atmosphere. For DMC development (i.e., for air parcels to reach their LFC), additional lift, moisture supply and instability are necessary. It is our purpose here to describe the mechanisms that enhance lifting along a UTMG, bringing air parcels beyond their LFC and favouring the transition to DMC.

UTMG correspond to moisture gradients in the satellite Water Vapour imagery and mark the boundaries of stratospheric dry intrusions. These features are well known and extensively described in the literature (initially by Rossby, 1938; Hoskins et al. 1985; Browning et al., 2000). Many names are given to this concept i.e. Tropopause folding, dry intrusion, Potential Vorticity Anomaly, PV-banner, dry slot, Water Vapour Black Stripe and many more. Usually, literature refers generally to cyclonic features in connection to extratropical cyclones or at the cyclonic side of a trough or cut-off low. These dry intrusions can also be fragmented and or advected, i.e. around a trough towards its anticyclonic forefront (Appenzeller et al., 1996)

In the following, we discuss a likely concept for the physical processes occurring along the UTMG. Most of the times, black stripes in the Water Vapour imagery of weather satellites can easily be identified by an elongated boundary and a significant decrease in Brightness Temperature, BT. According to textbook literature, PV anomalies greater than 2 PV units will occur at middle or even low levels of the troposphere below the area of WV black stripes. A propagating dry intrusion / black stripe is also an indicator for upper level divergence at its leading edge and hence a favourable location for lift at the mid tropospheric levels (Fig. 2, a). With the dry intrusion (black stripe) and the respective cooling of upper- and mid-levels, the horizontal gradient of the Θ_e lapse rates perpendicular to the UTMG also increases (Fig. 2, b). Antonescu et al. (2013) measured an increase of vertical wind shear in connection with tropopause folds. Santurette and Georgiev (2005) postulate a jet axis along the boundaries of the WV dark stripes (Fig. 2, c). Given the strong horizontal gradients of wind speed and Θ_e, the presence of symmetric or Conditional Symmetric Instability (CSI) becomes more likely near the UTMG (also Fig. 2 c.). Indicators for the existence of CSI would be negative Equivalent Potential Vorticity EPVg (McCann, 1995) and positive Symmetric Convective Available Energy SCAPE (see also Markowski, et al. 2005, 53pp).

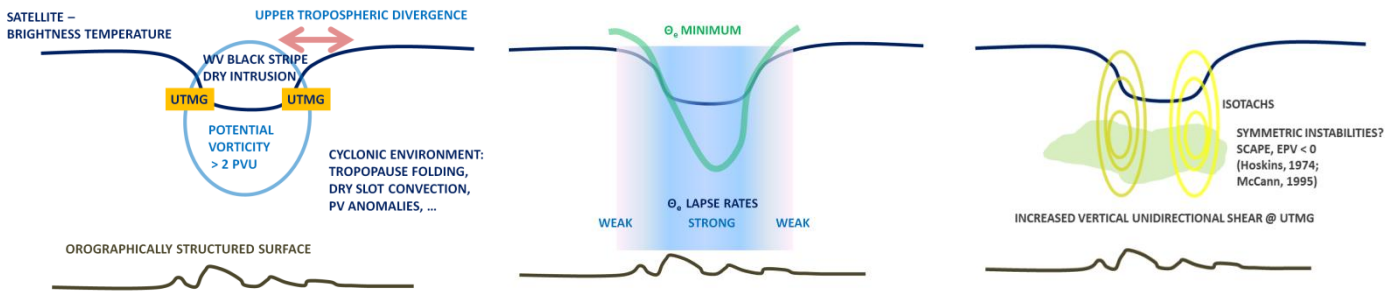

Fig. 2, a-c: Concept schematics described above

To show whether the coexistence of moist gravitational and moist symmetric instabilities along the UTMG provides additional lift at levels around the tops of shallow convective clouds, a case study has been performed with WRF model simulations in comparison to observed satellite imagery. If simulations prove to be reasonably accurate, the use of a numerical model allows analysing all the relevant diagnostic parameters and evaluating their importance towards convective development.

The case study of 2014 July 07

The area of interest over the eastern part of Austria is situated within a pressure ridge (see Fig. 3, overlay: ECMWF 500 hPa geopotential, orange lines). An approaching cold front is situated over Western Europe and the BENELUX

countries. Ridge cloudiness occurs between France, Switzerland and parts of Germany. The RGB imagery indicates shallow cloudiness over the mountainous area of the eastern alpine ridge (red) as well as a WV Black Stripe with corresponding UTMG stretching from Eastern Germany to Bosnia.

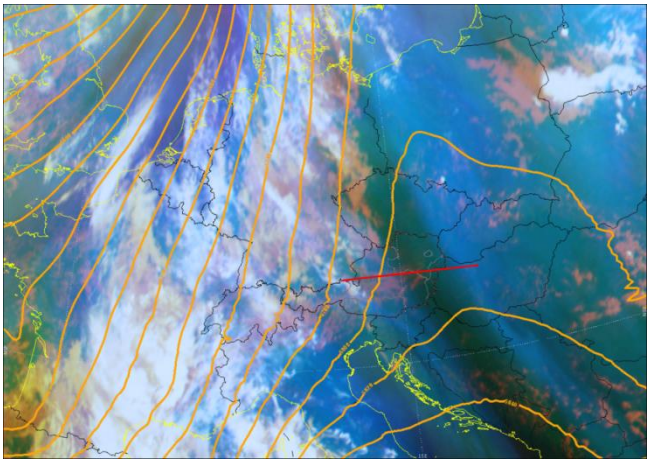

Fig. 3: 7 July 2014, 0900 UTC, MSG RGB Image composite: Low Clouds: IR 8.7µm (red); Mid Level Moisture: WV 7.3µm (green); High level Moisture: WV 6.2µm (blue), orange lines: 500 hPa Geopotential; red line indicating Vertical Cross Sections VCS of D1

WRF model setup

The WRF mesoscale numerical weather prediction model (Version 3.7), with the Advanced Research WRF (ARW) fully compressible and non-hydrostatic dynamical solver (http://www2.mmm.ucar.edu/wrf/users/model.html), was used for the simulations. The model uses a terrain-following, pressure-based vertical coordinate (eta-coordinate). The simulation was initialized 12 hours before the event took place and integrated over 1 day. It was performed with 3 nested domains with horizontal grid spacing of 20 km, 4 km and 0.8 km respectively, and 60 vertical levels with monotonically increasing thickness. The initial and boundary conditions for the integration were derived from ECMWF analysis data (6h temporal resolution). The positions of the computation domains are shown in Fig. 3.

For the parameterization of cumulus physics, a Grell 3D Ensemble Scheme is used for domain 1, while no parameterization is applied to domains 2 and 3. The other physical parameterization options, which are the same for each domain, are listed in Table 1. Only results from D1 and D3 are shown in what follows.

Planetary Boundary Layer	Mellor-Yamada-Janic Scheme
Microphysics	WSM-6 Scheme
Long-wave Radiation	RRTM Longwave Scheme
Short-wave Radiation	Simple Shortwave Scheme
Land Surface	Unified Noah Land Surface Model
Surface Layer	Eta Similarity Scheme

Table 1: Simulation parameterization options for all domains

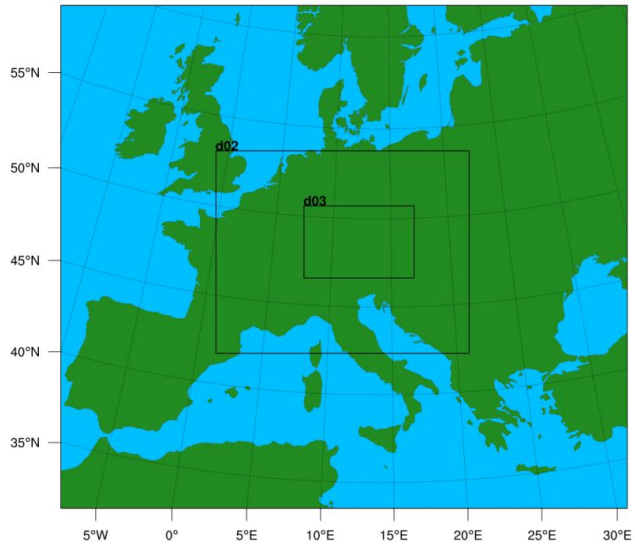

Fig. 4: Domains used for the WRF model simulation, D1 matching the image pane and D2 and D3

Discussion of the Satellite imagery, model simulations, their respective time increments and predictor parameters below the UTMG and their synoptic boundary conditions

The red line in Fig. 3 above indicates the location of the Vertical Cross Section VCS within the large domain D1 on 7 July 2014 at 0900 UTC. Comparing the satellite RGB composite from Fig. 3 and the VCS from Fig. 5a, the position of the dry intrusion is well reflected in the vertical distribution and the horizontal and vertical gradients of the Relative Humidity RH (dark blue shading), and the horizontal and vertical gradients of Θ_e (minimum between the levels of 800 and 500hPa). In Fig. 5b, a zone above 14E and between 700 and 500 hPa shows also significant gradients of the horizontal wind speed and hence an increase in vertical wind shear. Also a clear signal of negative EPV can be seen in the layer between 850 and 700hPa (Fig. 5b), reflecting the decrease of Θ_e with height. Thus, indicators for conditional instability (CI) and conditional symmetric instability (CSI) can be found coexisting below the western UTMG of the dark stripe.

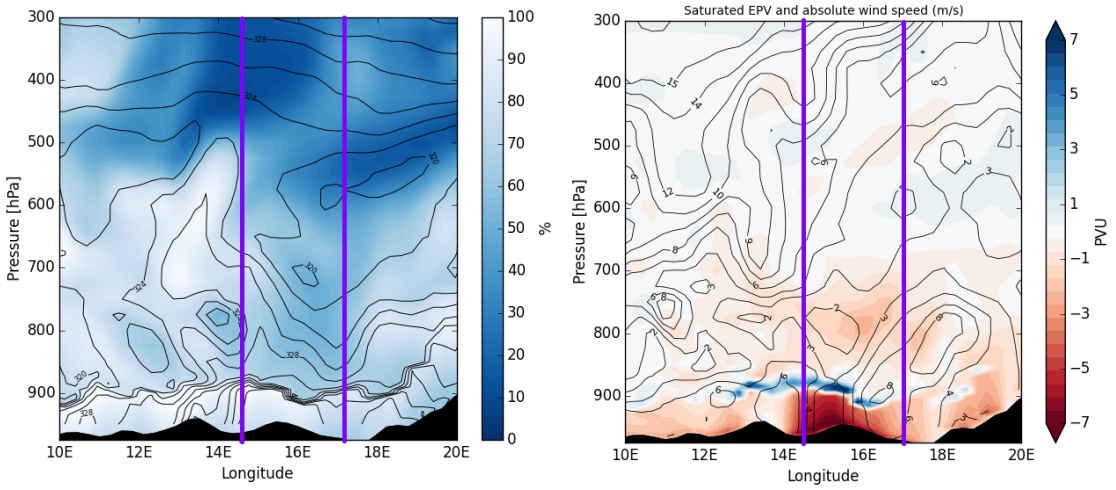

Fig. 5, a-b: 7 July 2014, 0900 UTC, WRF VCS, D1, resolution 20 km, position indicated on satellite image; Left: Relative Humidity [%] (shaded), Θ_e [K] (lines); Right: EPV [PVU] (shaded), Horizontal Wind Component [m/s] (lines); violet lines indicate the extent of the following VCS from the high resolving D3 in the WRF simulation

In the following, the VCS show time increments between 0800 and 1020 UTC, where the evolution from shallow convective cloudiness towards precipitating DMC in the vicinity of the UTMG parameters can be followed. The temporal evolution of convection in the WRF simulation is generally in very good agreement with satellite observations in this case. The horizontal distribution of EPV minima and SCAPE maxima from the WRF model near the regions of the first onset of DMC is also shown.

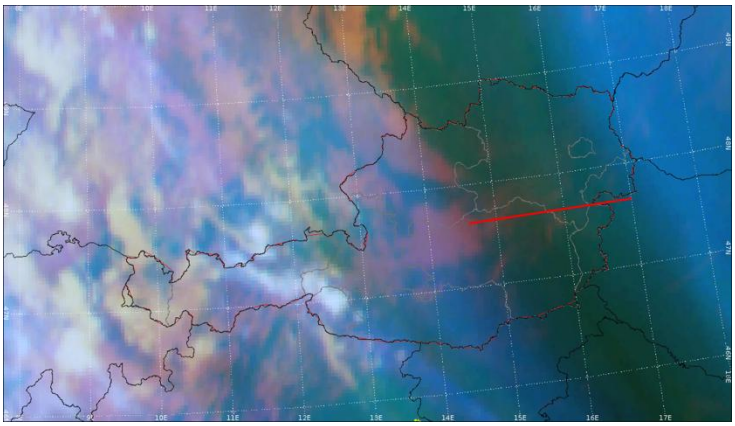

Fig. 6a: 7 July 2014, 08:00 UTC MSG RGB Image composite: Low Clouds: IR 8.7µm (red); Mid Level Moisture: WV 7.3µm (green); High level Moisture: WV 6.2µm (blue); Red Line: Position of the model simulation VCS, D3

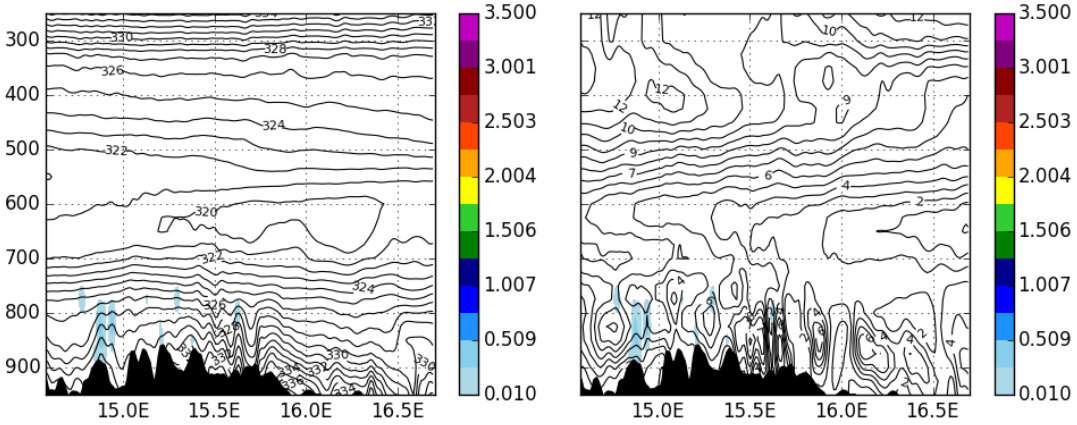

Fig. 6b: 7 July 2014, 08:00 UTC, WRF simulation D3, VCS:Total hydrometeor mixing ratio [g/kg]; q_h(shadings): sum of liquid cloud, rain, ice cloud, snow, and graupel water contents; Equivalent Potential Temperature Θ_e [K], (black lines, left side); horizontal component of true wind speed [ms^{-1}] (black lines, right side)

After 1 hour of development, the shallow convective clouds (red) become more pronounced in the satellite image (compare Fig. 6a and Fig. 7a). Also the WRF model simulation resolves convective saturated plumes growing toward the 700 hPa level between 08:00 and 09:00 UTC (Fig. 6b and Fig. 7b). The area below the UTMG around 15.5E around this level shows a decrease of the vertical Θ_e gradient. Additionally, the vertical wind shear becomes more pronounced.

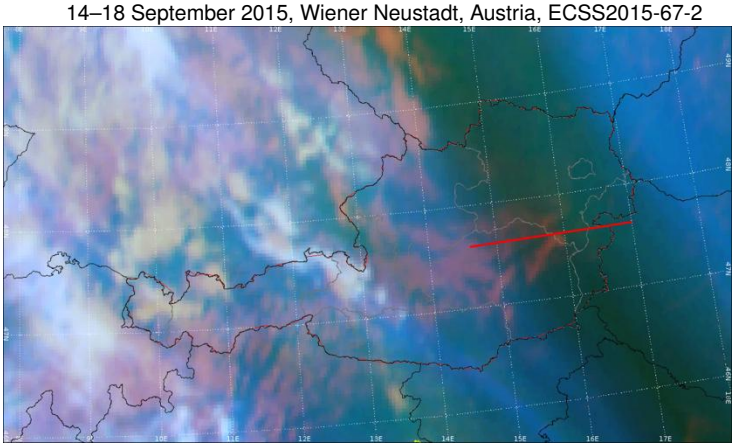

Fig. 7a: 7 July 2014, 09:00 UTC MSG RGB Image composite: Red Line: Position of the model simulation VCS, D3

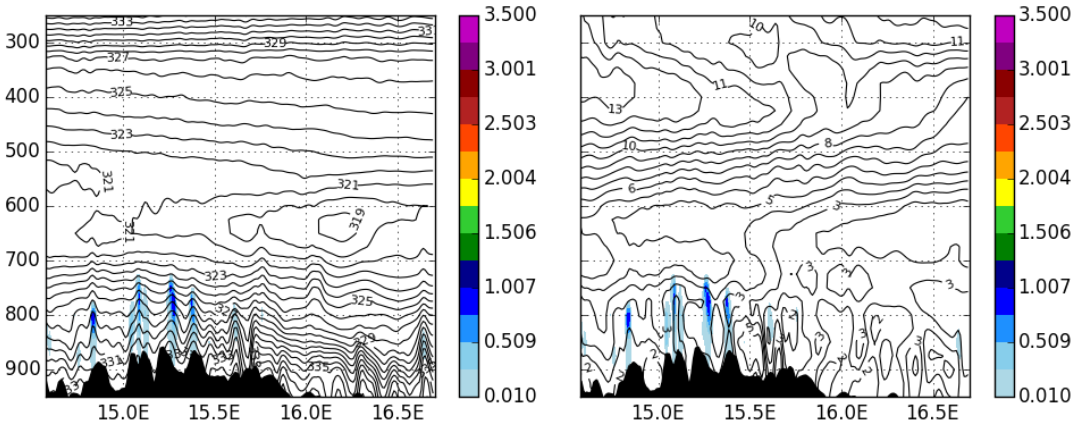

Fig. 7b: 7 July 2014, 09:00 UTC, WRF simulation D3, VCS:as above

One hour later, at 10:00 UTC, the appearance of a whiter shade at the position of the convective activity in the satellite RGB indicates further vertical growth of the convective updraft, representing a deeper saturation of the columnup to 500 hPa (Fig. 8a, and d-e).

In Fig. 8b the radio sounding of Vienna from the 7 July 2014 at 12:00 UTC is displayed. One significant characteristic in the vertical distribution of the relative humidity can be seen in the layer between 600 and 400 hPa, indicating the movement of the dry intrusion above the station. This property of the vertical moisture profile is representative of most investigated cases with convective initiation at UTMG (Krennert, et al., 2003). Significant signals can be also detected from the vertically integrated quantities of the negative EPV and SCAPE around the area of interest above the eastern part of Austria at this time step, indicating a high probability of the existence of CSI (Fig. 8, f-g).

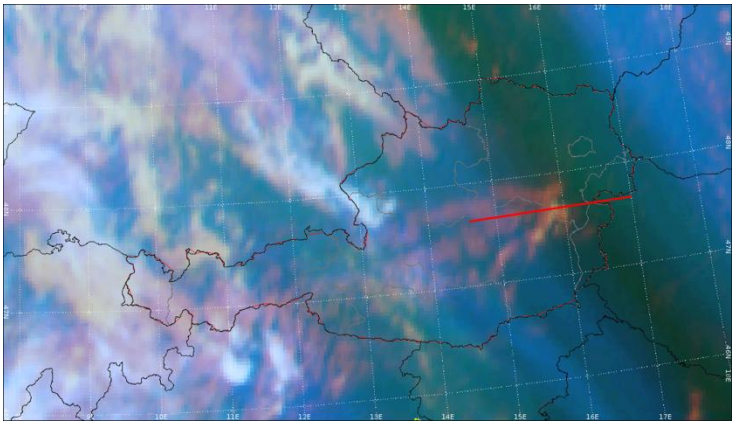

Fig. 8a: 7 July 2014, 10:00 UTC MSG RGB Image composite: Red Line: Position of the model simulation VCS, D3

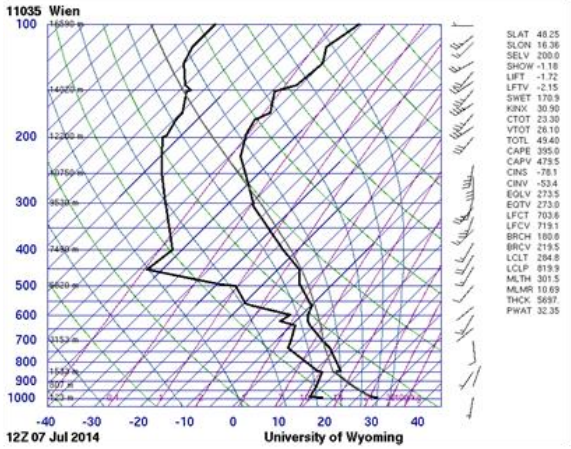

Fig. 8b: 7 July 2014, sounding Vienna 12:00 UTC; the level of the LFC is located around 700hPa

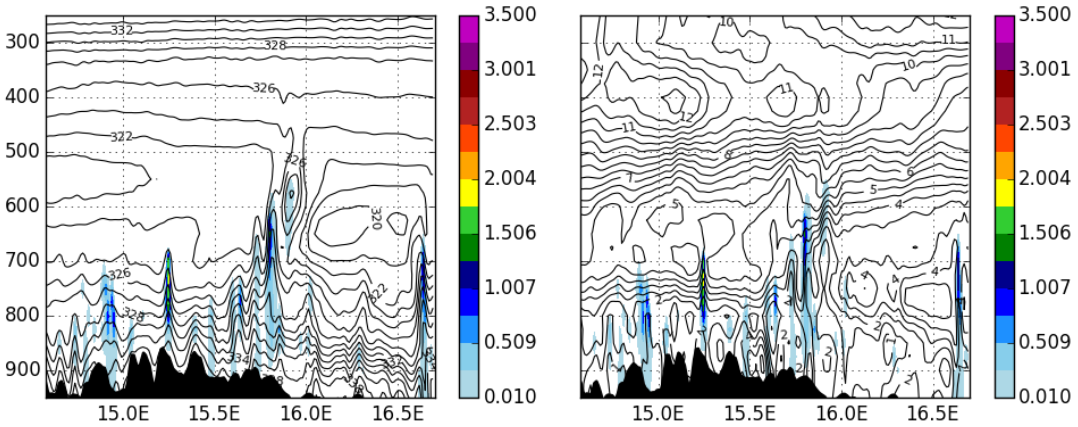

Fig. 8, d-e: 7 July 2014, 10:00 UTC, WRF simulation D3, VCS:as above

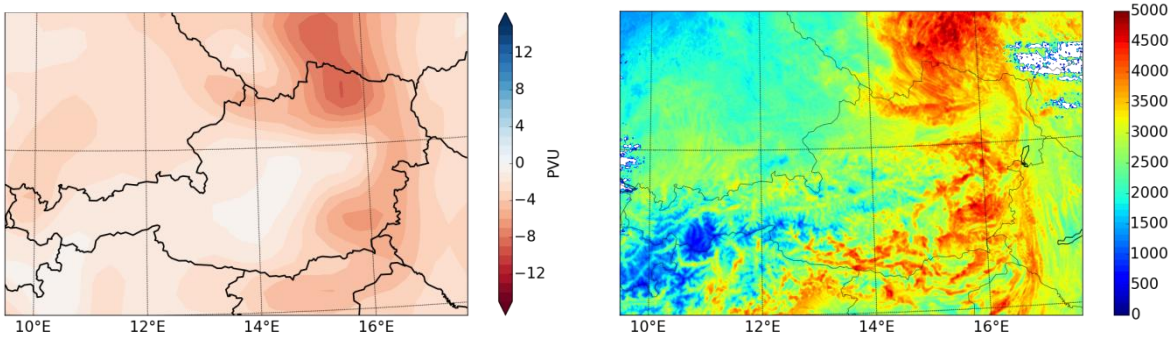

*Fig. 8, f-g: 7 July 2014, 10:00 UTC: Left WRF simulation D1: Negative EPV saturated [PVU = 10^{-6}*K*m^2/kg*s], horizontal minimum projection, layer between 850 and 700 hPa; Right, WRF simulation D3: Symmetric Available Potential Energy SCAPE [J/kg], integrated from 950 hPa, calculated after Dixon (2000)*

Resulting DMC in satellite imagery and WRF model simulations

Twenty minutes later, at 10:20 UTC, the satellite imagery and the model VCS depict a fully grown DMC in its maturing state.

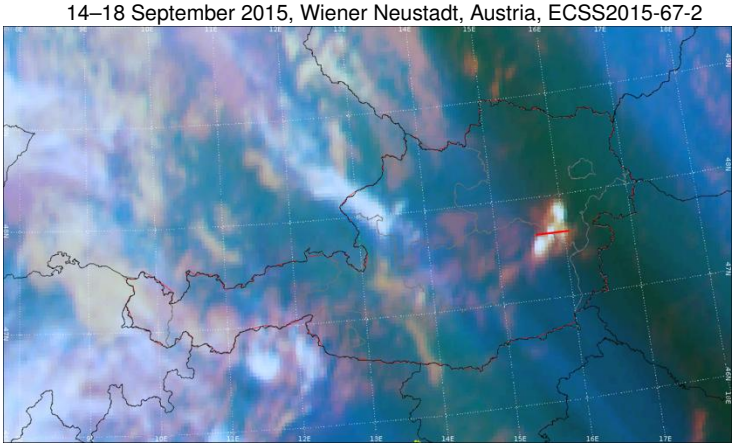

Fig. 9a: 7 July 2014, 10:20 UTC MSG RGB Image composite: Red Line: Position of the model simulation VCS, D3

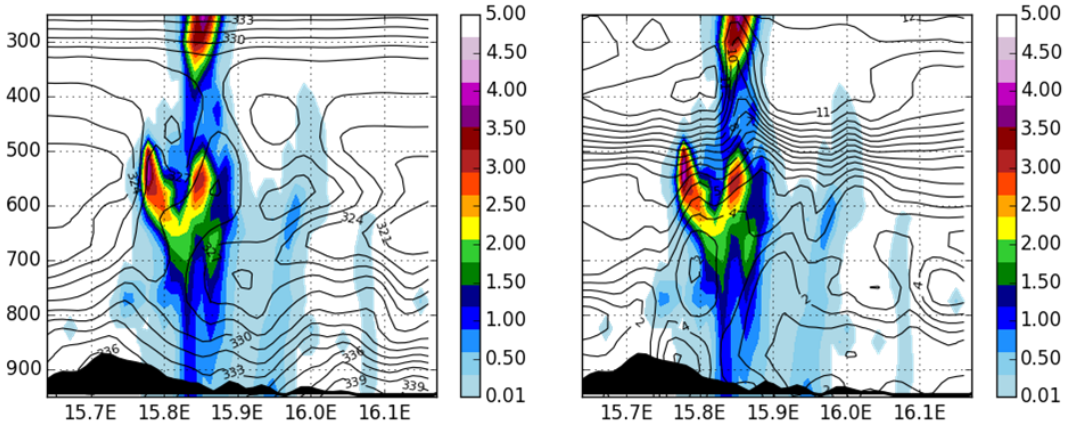

Fig. 9b: 7 July 2014, 10:20 UTC, WRF simulation D3, VCS: as above

Concluding remarks for the case study of 7 July 2014:

The connection between the UTMG of Water Vapour dark Stripes / dry intrusions and the preferred initiation of DMC along these boundaries was investigated in the representative case study of 7 July 2014. On the basis of a WRF model simulation, it was shown that the DMC development took place in the vicinity of pronounced horizontal and vertical Θ_e gradient and wind shear.

These, and the existence of distinct values of SCAPE and negative saturated EPV atlower mid–levels of the troposphere, respectively, make the coexistence of CI and CSI along the UTMG plausible. All ingredients of CI and CSI are available within a layer between 900 and 700hPa before shallow convective towers reach these levels, prior to DMC evolution. The release of SCAPE within a shallow tropospheric layer between 850 and 700hPa possibly enables slantwise convection, adding further lift (although in the magnitude of cm/s, Schultz, et al., 1999) for the air parcel to reach its LFC.

Xu (1986) distinguishes two different types of coexistence between gravitational and symmetric instability, corresponding to two distinct mechanisms for the release of symmetric instability leading to slantwise convection. The “upscale development” describes the case where “smallscale moist gravitational convection develops first, followed by mesoscale banded organization of clouds due to the release of symmetric instability” (Schultz, et al., 1999). Morcrette, et al., 2006, and Fantini, et al., 2011 also describe this effect in more detail. On the contrary, the ‘‘downscale development’’ defines “an ascent in a moist symmetrically unstable environment, leading to latent-heat release, effectively destabilizing the midtroposphere to gravitational convection”.

The mid–tropospheric slantwise convection mechanism described in our case study seems to be similar to the "downscale development" scenario. That is, the presence of a state of conditional symmetric instability in the upper troposphere appears to favour the transition from shallow to deep convection. However, decisive evidence in support of this hypothesis is still missing, and will be sought in future research efforts by analysing the balance of forces acting on air parcels along their lagrangian trajectories through the main convective updraft.

References:

Appenzeller, C., Davies, H.C., Norton, W.A., 1996: Fragmentation of stratosphericintrusions. Journal of Geophysical Research 101, 1435–1456.

Antonescu, B., Vaughan, G., Schultz, D. M.,2013: A Five-Year Radar-Based Climatology of Tropopause Folds and Deep Convection over Wales, United Kingdom. Mon. Wea. Rev., 141, 1693–1707.

Browning, K. A., Thorpe, A. J.,Montani, A.,Parsons, D.,Griffiths, M.,Panagi, P.,Dicks, E. M.,2000: Interactions of Tropopause Depressions with an Ex–Tropical Cyclone and Sensitivity ofForecasts to Analysis Errors, Mon. Wea. Rev., 128, 2734pp

Fantini, M., Malguzzi, P., and Buzzi, A., 2012: Numerical study of slantwise circulations in a strongly-sheared pre-frontal environment, Q. J. Roy. Meteor. Soc., 138, 585–595

Dixon, R. S., 2000: Diagnostic studies of symmetric instability, PhD thesis, University of Reading

Hoskins, B.J., McIntyre, M.E., Robertson, A.W., 1985: On the use and significance ofisentropic potential-vorticity maps. Quarterly Journal of the Royal MeteorologicalSociety 111, 877–946. Corrigendum 113, 402–404.

Krennert, T., Zwatz-Meise., V., 2003: Initiation of Convective Cells in Relation to Water Vapour Boundaries in Satellite Images. Atmos. Res. 67-68, 353-366.

Markowski, P., Richardson, Y., 2010: Mesoscale Meteorology in Midlatitudes, 183pp, Wiley

McCann, D.W., 1995: Three Dimensional Computations of Equivalent Potential Vorticity, Weather and Forecasting, 10, 798–802

Morcrette, C.J., Browning, K,A,. 2006: Formation and release of symmetric instability following Delta-M adjustment. Q. J. R. Meteorol. Soc. 132: 1073–1089

Rossby, C. G., 1938: On the mutual adjustment of pressure and velocity distributionsin certain simple current systems, II. Journal of Marine Research 2, 239–263.

Santurette, P., Georgiev, C. G., 2005: Applying Satellite Water Vapour Imagery and Potential Vorticity Analysis, Weather Analysis and Forecasting, Elsevier

Schultz, D.M., Schumacher, P.N., 1999: The use and misuse of conditional symmetric instability. Mon. Weather Rev. 127: 2709–2732.

Xu, Q., 1986: Conditional symmetric instability and mesoscale rain bands, Quart. J. Roy. Meteor. Soc., 112, 315–334.